Seismicity and Seismotectonics in Epirus, Western Greece: Results from a Microearthquake Survey

by G-Akis Tselentis, Efthimios Sokos, Nikos Martakis, and Anna Serpetsidaki

Abstract   During a twelve-month passive tomography experiment in Epirus, in northwestern Greece, a total of 1368 microearthquakes were located. The most accurately located events and focal mechanisms are used here to understand the seismotectonics of the area. The seismicity shows a clear association with the main, previously defined deformation zones. A total of 434 well-defined focal mechanisms were also used for the determination of the stress pattern in the area. The computed stress-field pattern is quite complex close to the surface and almost homogeneous at depths below 15 km. For these depths, the stress field is purely compressional in a west-southwest direction, whereas for shallow depths it is transpressional or even extensional for some smaller areas. The abrupt change in the stress pattern, which occurs as depth increases, suggests the existence of a detachment surface, which is provided by the evaporites that have intruded into the upper layers through the thrust zones. The presence of the evaporites and their lateral extent is mapped by the seismicity distribution and confirmed by seismic tomography. Based on the findings, we estimate a possible total evaporite thickness of almost 10 km at least for the central part of the study area. Such a result is important for the oil exploration efforts that have just started in Epirus.

Introduction

Epirus is located on the northwestern edge of Greece. It is a key area for various geodynamical models that have been proposed for the Aegean because it is the region where the transition of the extensional Inner Aegean regime to the compressional outer Aegean takes place. This transition is mapped on the basis of faulting which varies from thrust and strike slip to normal (Mercier *et al.*, 1972; King *et al.*, 1983; Doutsos *et al.*, 1987; Underhill, 1989; Hatzfeld *et al.*, 1995; Waters, 1994).

The main tectonic structures are thrust belts that trend north-northwest as a result of east–west shortening (Taymaz *et al.*, 1991) and are cut by almost perpendicular strike slip or normal faults. According to Hatzfeld *et al.* (1995), compression in Epirus is most likely due to the jump of active thrusting from the Pindos to the Ionian zone and continues to the present. The main geotectonic zones are the Ionian, the Gavrovo, and the Pindos zones (Aubouin, 1959; Jacobshagen, 1986). Starting from the eastern end, the Pindos zone is thrusted on the Gavrovo zone and the Gavrovo on the Ionian zone (Fig. 1). Smaller minor thrusts exist, such as the Internal and Middle Ionian thrust (Avramidis *et al.*, 2000) along with strike-slip faults of transfer character (IGSR and IFP, 1966; Waters, 1994).

Previous microearthquake studies in the Epirus have been conducted by King *et al.* (1983), Kiratzi *et al.* (1987), Waters (1994), and Hatzfeld *et al.* (1995), whereas geolog-ical and geomorphological work was performed by IGSR and IFP (1966) and King *et al.* (1993). During these studies, the major deformation zones were pinpointed and the first results on the geodynamics of Epirus were obtained. These results support east-northeast–west-southwest shortening, compatible with the continental convergence west of Corfu and north-northwest extension, further east, close to the Pindos foothills (Hatzfeld *et al.*, 1995). Papazachos and Kiratzi (1996) studied the crustal deformation of the whole Aegean area and obtained similar results. In addition, King *et al.* (1983) used geomorphological data and boundary-element modeling and proposed the existence of a substantial left-lateral strike-slip component in addition to the compressional motion.

In this article we present high-quality seismological data for the area of Epirus. The recorded seismicity delineates the zones of present active deformation. By using fault-plane solutions, the stress distribution in the area is determined and results about its seismotectonic regime are derived. In addition, the seismicity distribution is used to assess the thickness and the lateral extent of a possible evaporite layer.

Seismograph Network and Data

A portable network of 40 stations was installed in the area for 12 months (August 1998–July 1999) (Fig. 2). The
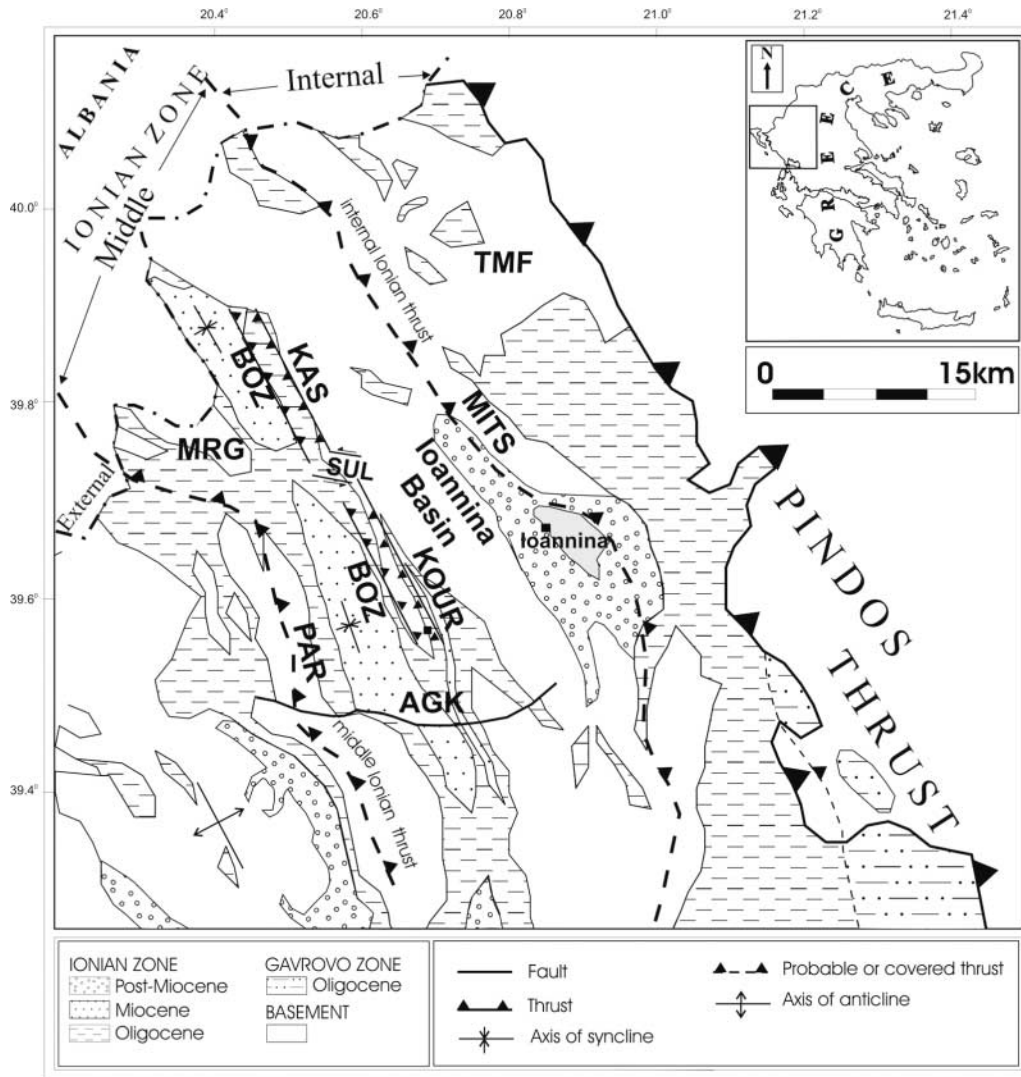
Figure 1. Simplified geological map of western Greece, depicting the main isopic zones. Modified after IGSR and IFP (1966) and Avramidis *et al.* (2000). PAR, Paramythia; KOUR, Kourendon; SUL, Soulopoulo; KAS, Kassidiares; MRG, Mourgana mountain; BOZ, Botzara; TMF, Timfi.

station spacing was chosen to be less than 10 km to have reliable focal-depth estimation. Each station was equipped with a three-component 4-Hz SIG borehole sensor, a 24-bit Earth Data recorder, and a Global Positioning System (GPS) unit. The instruments have flat transfer function for velocity in the frequency range from 1 Hz to 50 Hz. The recording was continuous with a sampling frequency of 100 Hz. Every 15 days data were collected and stored in an 80-Gb hard disk. A special program was developed, based on the STA/LTA (short-term average/long-term average) algorithm, to identify events, merge event files, and store them on a tape. A minimum number of eight stations was used as a criterion for the event selection.

During the operation of the network a total of 1368 earthquakes were recorded. The initial hypocentral locations were determined by using the program HYPO71 (Lee and

Lahr, 1975; Lee and Valdes, 1985). The velocity model adopted for this procedure was derived by 1D inversion using the VELEST software (Kissling *et al.*, 1994) and it is presented in Table 1. From this catalog we selected 434 events having more than 15 arrivals (*P* and *S*) and epicenters within the network. The local magnitudes M_L of these events are within 1.11 and 3.2, whereas their depths vary between 1 and 35 km. (Figs. 3 and 4). The magnitudes were computed using the coda duration method (Lee *et al.*, 1972), with the same parameters used in the routine processing of PATNET (PATras NETwork) records for western Greece (Tselentis *et al.*, 1996). The high quality of this dataset is attested to by the formal hypocentral errors, which are smaller than 0.8 km and by the adequate azimuthal coverage (largest azimuthal gap <180°).
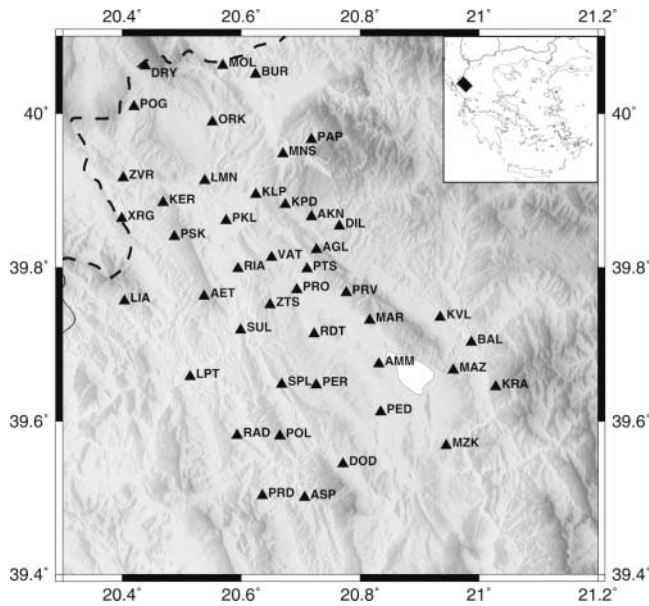
These selected events were used in a 3D tomographic

Figure 2.   Map of the seismological stations installed during the experiment.

Table 1
The Velocity Model Derived Using 1D Inversion

Depth (km)	Velocity (km/sec)
0.0	5.12
2.0	5.33
4.0	5.52
6.0	5.62
8.0	5.82
10.0	6.05
15.0	6.25
20.0	6.39
40.0	8.0

study using the program *Simulps12* (Thurber, 1986), the results of which will be presented elsewhere. In this article we use the 3D relocated epicenters and the focal mechanisms, as determined by the tomographic inversion, to study the seismotectonics of the area. The majority of the relocated events have location error less than 0.5 km and root-mean-square (rms) residuals less than 0.08 sec.

The fault-plane solutions were determined using the FPFIT program (Reasenberg and Oppenheimer, 1985), with the azimuth and angle of incidence computed during the tomography inversion (Fig. 5). Of the 434 events, 270 events have more than 15 *P*-wave first arrivals, and 65% of them had more than 20 *P* readings. Most of the solutions (90%) were unique. For the events with multiple solutions we selected the ones with the highest quality, as estimated from the uncertainty measurements determined by FPFIT. The nodal planes are well constrained and the errors in strike, dip, and rake are less than 10°.

Of particular interest is the observation of various types of focal mechanisms. This is in good agreement with field observations within the Epirus region, as normal, reverse, srike-slip, and oblique-surface structures can be observed close together. A characteristic of oblique systems is the presence of slip partitioning and multiple mechanisms. Deschamps and King (1984) pointed this out for the Irpinia region, and Amelung and King (1997) pointed this out for central California.

The computed fault-plane solutions were used in a stress-tensor inversion with the method of Gephart and Forsyth (1984) and Gephart (1990). The methodology is described in the Stress-Tensor Inversion section

Seismicity

The recorded seismicity is presented in map view (Fig. 3) and in 3D view (Fig. 4). In general, the seismicity is concentrated in small clusters, while some scattered epicenters also exist, mainly at the northeast part of the area (TMF). The earthquake depth clearly increases toward the east in agreement with the Hatzfeld *et al.* (1995) observations (Fig. 3b). One striking feature of the spatial distribution of the epicenters is the large seismicity gap at midcrustal depths between the Kourenton-Kasidiares (KOUR-KAS) and the Mitsikeli (MITS) thrust (Fig. 3 area E). This gap is probably related to the presence of a large evaporite body (grayed volume in Fig. 3b) that has intruded into the upper layers through the Mitsikeli thrust surface.

Other features of the seismicity distribution are three clusters of epicenters west of the Kourenton-Kasidiares (KOUR, KAS) thrusts (Fig. 3, area B), two clusters of very shallow earthquakes (Fig. 3, area E), probably related to the evaporite presence close to the surface, and two clusters of relatively deep earthquakes (Fig. 3, areas C and D), which are the deepest recorded events. These deep clusters could be related to the major thrusts of the area (probably the middle Ionian; Fig. 1) that is still active today. This assumption is suggested also by the focal mechanisms of these events that are all of thrust type (Fig. 5).

In the southwest part of the study area (denoted by A in Fig. 3) we observe scattered seismicity south and north of the fault zone formed by the Agia Kyriaki fault and several smaller faults. The Agia Kyriaki fault (AGK) has been identified by IGSR and IFP (1966), Hatzfeld *et al.* (1995), and Boccaletti *et al.* (1997). It is characterized as an active structure, although Hatzfeld *et al.* (1995) did not record any significant seismicity related with this fault. The fault has a total length of 50 km and cuts across the major mountain ranges of Paramithia and Tomaros (Boccaletti *et al.*, 1997). These authors state that the fault is composed of several branches locally bifurcating and extends eastward from the Ionian coast to the Ioannina plain. Hatzfeld *et al.* (1995) proposed a left-lateral strike-slip motion for this fault, whereas Bocaletti *et al.* (1997) described the fault as a more
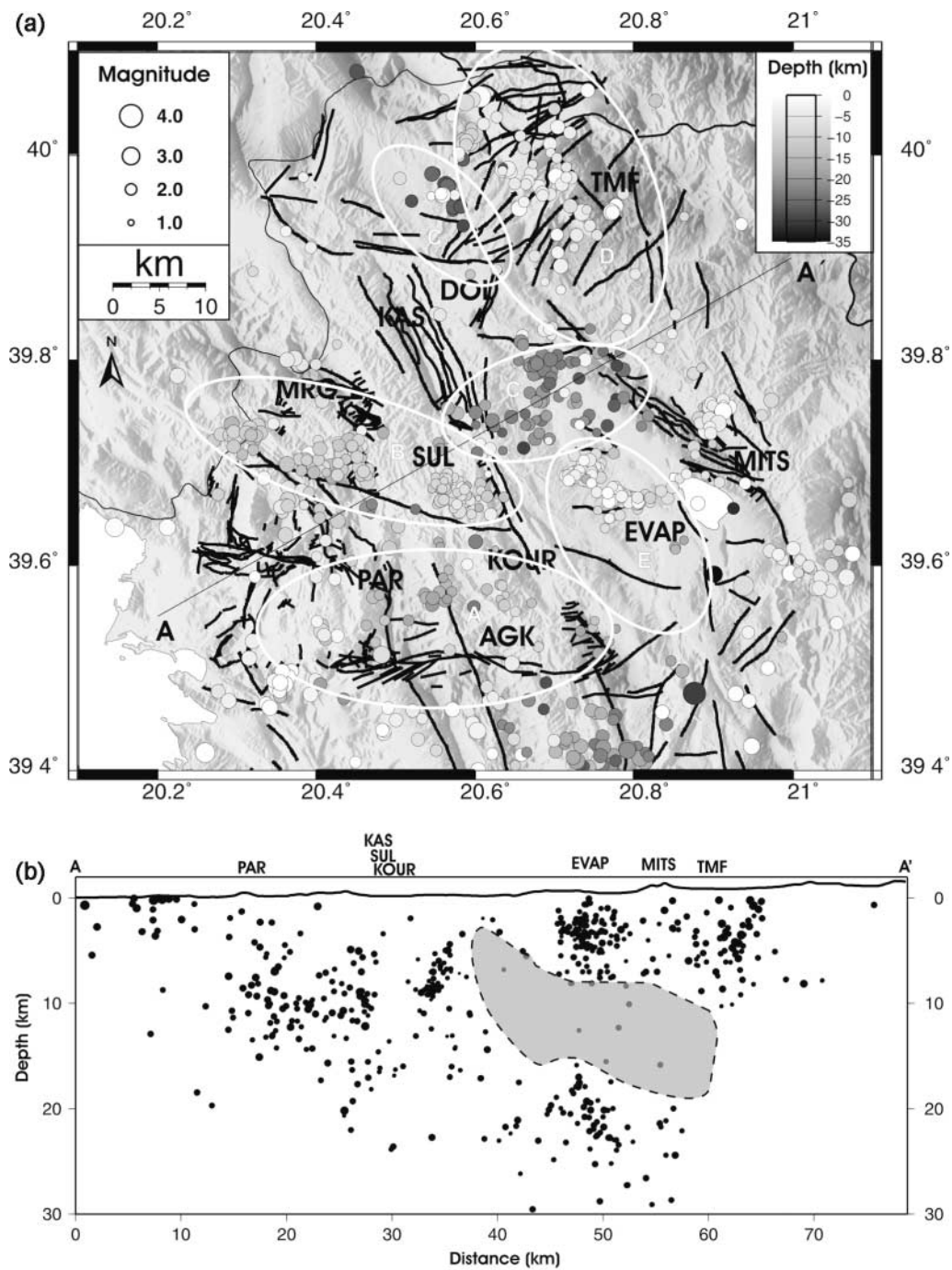
Figure 3. (a) Seismicity map of the 434 selected events that were used in the tomographic study of the area. Fault lines are taken from IGMR (1988), IGMR (1967b, c), IGRS and IFP (1966), Boccaletti *et al.* (1997), and Waters (1994). The dashed line is the Greek-Albanian border. PAR, Paramythia; AGK, Agia Kyriaki; KOUR, Kourendon; SUL, Soulopoulo; KAS, Kassidiares; DOL, Doliana; MRG, Mourgana mountain; EVAP, evaporite outcrop; TMF, Timfi; MITS, Mitsikeli. (b) Seismicity cross section across the study area; the gray-shaded area defines the main evaporite body.
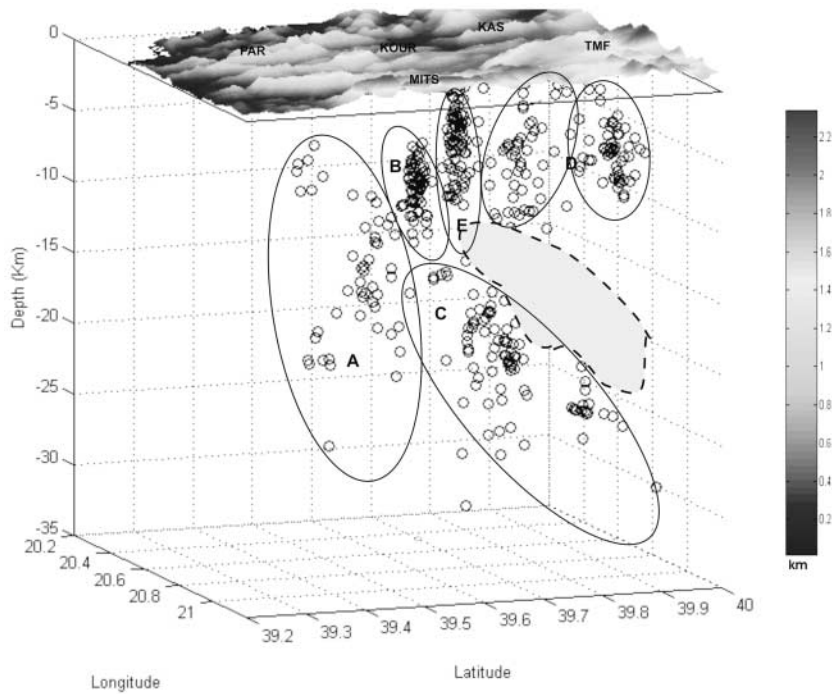
Figure 4.   Three-dimensional view of the seismicity distribution. Letters define the main seismic zones as discussed in the text.
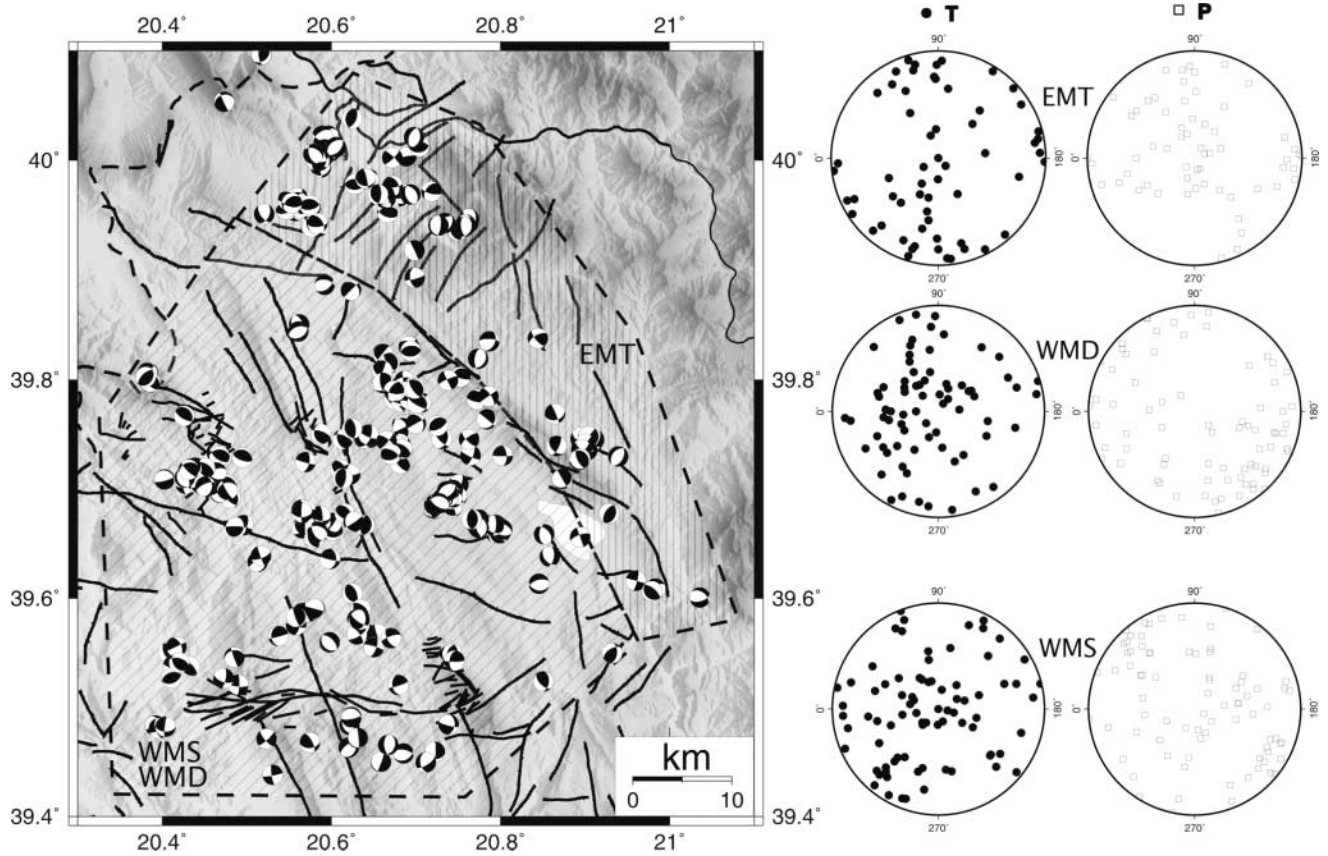

Figure 5.   Map of the fault plane solutions for the 270 events (lower-hemisphere projection, compressive quadrant shaded) and lower-hemisphere equal-area projection of P (pressure) and T (tension) axes. Hatched areas (EMT, WMS) correspond to the regions used in stress-tensor analysis. The WMD area is identical with WMS but for earthquake depths greater than 15 km.

complex left-lateral strike-slip deformation zone consisting of smaller faults that could form local negative and positive flower structures. The seismicity (Fig. 6) is distributed around the mapped fault traces without a prominent association with any of them. The depth of the earthquakes changes along the strike of the fault, with the seismicity relatively shallow (<12 km) at the west end, and mostly deeper than 12 km at the east end.

In the western part of the study area, which is referred to as the Paramythia-Mourgana area (Fig. 3, area B), the seismicity is concentrated in three main clusters. This area is bounded by the Kasidiares-Kourenton thrusts (Fig. 3, KOUR-KAS) in the east, and the Mourgana-Paramythia (MRG-PAR) thrust in the west (Figs. 3 and 7). The Botzara syncline (Fig. 7, BOZ), formed mainly by flysch deposits, is in the middle of these thrusts (Figs. 1 and 7). Smaller structures of oblique type also exist, like the Soulopoulo (SUL) gap, a system of oblique normal faults (Figs. 1, 3, and 7), which shifts the Kasidiares-Kourenton thrusts to the west (IGSR and IFP, 1966, King *et al.*, 1993).

The western cluster is close to the Greek-Albanian border and its seismicity lies between 5 and 14 km depth. We could not determine reliable fault-plane solutions for this cluster, but geological data for this area (IGSR and IFP, 1966) indicate the existence of normal to oblique faults that could easily explain the observed seismicity pattern (Fig. 7).

Another cluster of seismicity is located further east, close to the Soulopoulo gap (Fig. 7, SUL). This cluster has been described by Hatzfeld *et al.* (1995); they suggest normal faulting with a slight-strike slip component and a depth range of 5 to 8 km for the earthquakes in this area. According to our results, seismicity depth ranges from 2 to 10 km, whereas the type of faulting varies significantly, from oblique-normal to pure strike slip and even the reverse for some earthquakes. This variation of focal mechanisms implies the existence of a system of faults and it additionally suggests the existence of two main groups of faults, although they are not very well separated. These are a group of oblique to normal faults that trend north-northwest–south-southeast and a group of almost vertical reverse fault of north–south trend (Fig. 7). Oblique faults of similar trends have been mapped in this area by IGSR and IFP (1966), and the reverse fault could be the Kourenton fault, which has been described as backthrust by IGSR and IFP (1966).

The third cluster lies in the area between the previous two, just at the southern end of mountain Mourgana (MRG). The earthquakes in this cluster are located at the same depths as the other two. Because, enough geological information is not available for this area, a possible explanation for the seismicity distribution could be that in this area faults of northeast and northwest–southeast orientation exist. This is reasonable to assume, because these types of faults are present east and west of this area (Fig. 7). Fault-plane solutions are variable, with strike-slip and normal-oblique mechanisms along with some reverse mechanisms at about 12 km depth that could be connected with the middle Ionian thrust

(PAR) that is mapped farther west (Fig. 1) (IGSR and IFP, 1966).

The southeast part of the study area (Fig. 3, area E) that lies between the Mitsikeli (MITS) and Kourenton thrust is called Ioannina basin by King *et al.* (1993) (Fig. 1). The most remarkable features of the seismicity distribution in this area is the presence of two well-defined shallow clusters (Figs. 4 and 7, EVAP), a few kilometers west of the city of Ioannina, and the abrupt change of the seismicity depth just to the north of these clusters (Fig. 4). More than 250 earthquakes with magnitudes less than 3.0 define these two clusters (Figs. 4 and 8). The depth of the earthquakes in the clusters is practically limited to no more than 5 km, with just a few deeper events. All the computed fault-plane mechanisms are of normal type and the main fault orientations are northwest–southeast, with faults dipping to the southwest or northeast. It seems that these earthquakes are produced by a set of conjugate normal faults (Fig. 8), which are structures that can develop on top of evaporite domes.

These sets of faults, along with the absence of seismicity below the depth of 5 km, indicate that in this area a large evaporite body is close to the surface and extends to the north where no seismicity can be observed over a depth range of 15 km, as we can see in Fig. 3. This idea is also supported by the presence of an evaporite outcrop close to the two clusters and by additional information from geophysical and geological data (E. Karagiorgi, personal comm., 2001; IGMR, 1967a).

A possible estimation of the main evaporite body thickness, as seen on Figures 3b and 4, could reach 10 km or even more for the Ioannina basin area. This is an estimation based exclusively on the seismicity distribution because there are no geological reports for the thickness of the evaporites in this area. A comparable thickness has been reported for the Dumrea evaporite structure in Albania, which has a drilled thickness of 5.6 km and forms a giant sheath fold (Velaj *et al.*, 1999). Moreover, the same authors report that the evaporites have been duplicated by thrusting and the evaporite sheets have been thickened and folded. Based on these results, an estimate of 10 km thickness for the Ioannina evaporite seems reasonable because the geological structures in Albania extend south to Epirus and Western Greece. These conclusions are in agreement with the results of the tomographic inversion and are depicted in Figure 9, which presents a horizontal seismic velocity section at the depth of 1 km and the corresponding vertical seismic velocity section along line AA′ with depth.

East of the Soulopoulo gap (SUL) and the Kasidiares (KAS) thrust (Figs. 3 and 4, area C), a remarkable change in the depth of the seismicity can be observed. The depths of the earthquakes in this area range from 15 to 30 km, in contrast to the depth of the earthquakes further west, which is up to 20 km, and most of the earthquakes are even shallower (<15 km). A similar deepening of the hypocenters was observed by Hatzfeld *et al.* (1995). The seismicity is limited to two deep clusters and a narrow zone that extends
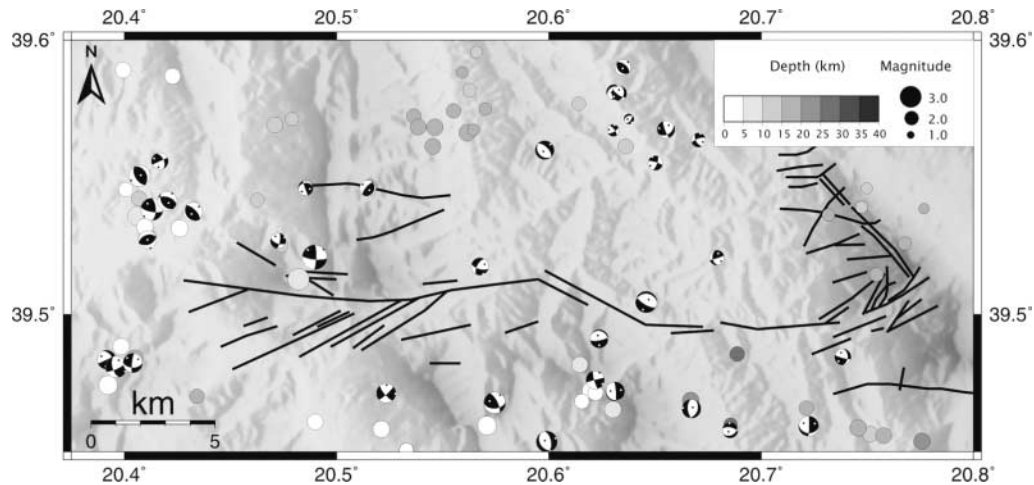
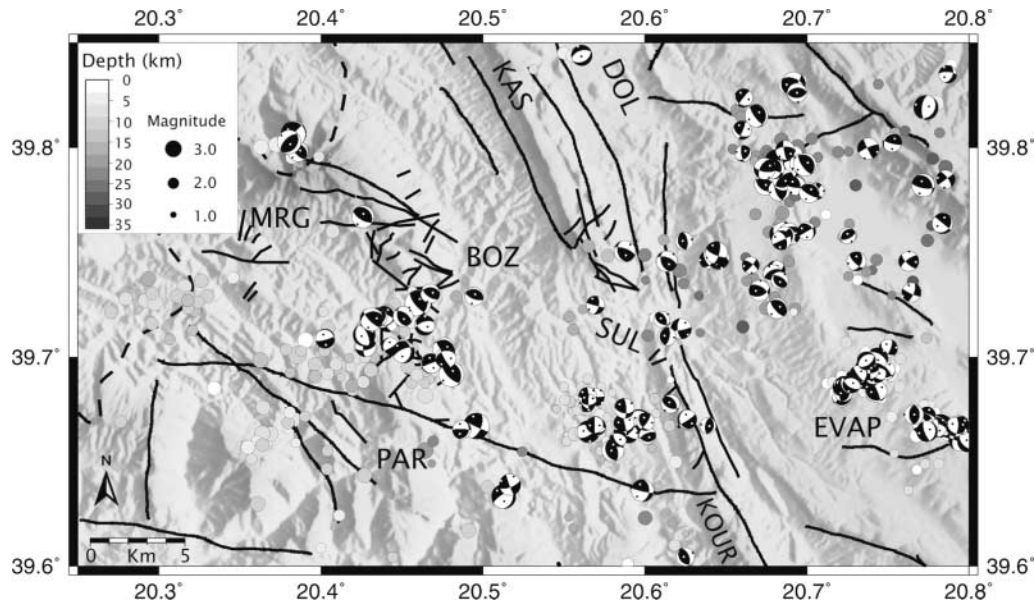Figure 6.   Seismicity and focal mechanisms in the Agia Kiriaki fault area.

Figure 7.   Seismicity and focal mechanisms in the Paramythia-Mourgana area. PAR, Paramythia; KOUR, Kourendon; SUL, Soulopoulo; KAS, Kassidiares; MRG, Mourgana, mountain; DOL, Doliana; EVAP, evaporite field. Fault lines are drawn according to IGMR (1988) and IGRS and IFP (1966). The dashed line is the Greek-Albanian border.

to the east from the Soulopoulo gap. These clusters are separated by 15 km (Fig. 10) and have similar pure reverse faulting focal mechanisms, which means that they probably belong to the same thrust or to two thrusts of the same orientation.

Besides the above two clusters there is also a narrow seismicity zone in the Ioannina basin, almost 7 km wide, that extends to the east from the Soulopoulo gap (Fig. 10). Seismicity in this zone starts at 15 km depth and continues up to 24 km. Fault-plane solutions for these earthquakes suggest reverse faulting in a north-northwest–south-southeast direction and strike-slip faulting in an east–west direction, respectively. The origin of this zone is not clear but it is

probably due to the intersection of the southern part of the Kasidiares transpressional structure and the Soulopoulo strike-slip zone.

A significant number of earthquakes are located in the area D of the mountain Timfi (TMF) (Fig. 3). In this area no microearthquake data have been reported, before this study, but it is believed to be an area where extension is taking place (Papazachos and Kiratzi, 1996). The earthquake foci are quite shallow with their depth ranging from 3 to 15 km. Although the existence of one or two active faults seems to be suggested by the microseismicity distribution, the epicenters cover the whole area, thus suggesting the existence of an active fault system (Fig. 10). The majority of
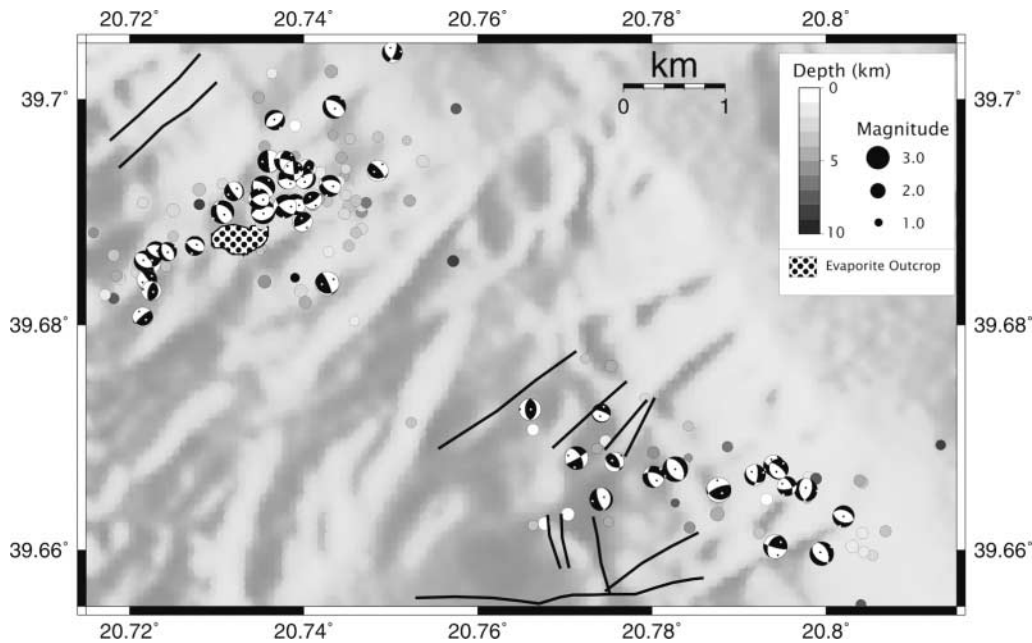
Figure 8.   Seismicity and focal mechanisms in the area of the two evaporite-induced clusters (evaporite outcrop and minor faults are drawn according to IGMR [1967a]).

the fault-plane solutions strike north-northeast, whereas a few mechanisms have a clear north–south strike. The Timfi area is the only area in Epirus with such a clear extensional character, if we exclude the two clusters in the Ioannina basin. It seems that this extensional character is connected with the collapse of the thrust fronts that have propagated to the west. These results are in agreement with those of Doutsos and Koukouvelas (1998).

Finally the northwest part of the study area, the Doliana (DOL) basin (Fig. 3) (King *et al.*, 1993) is the area with the lowest recorded seismicity. Just a few sparse epicenters were located in the basin and there is almost no seismicity that could be connected with major structures like the Doliana left-lateral strike-slip fault or the northern part of the Kasidiares thrust. These are the basin's northern and western boundaries and, according to King *et al.* (1993), should be active.

Stress-Tensor Inversion

Method

We computed 270 well-constrained focal mechanisms for the area. This is the best available dataset for this part of Greece so far. The focal mechanisms reveal a complicated stress field where both normal and reverse faulting are present in adjacent areas (Fig. 5). The focal mechanisms were determined using the method of Gephart and Forsyth (1984), which is based on the assumption that the deviatoric stress tensor is uniform over the study area. Other assumptions of the method are that the slip vector of any focal mechanism points to the direction of the maximum resolved shear stress

on the fault plane (Bott, 1959) and that the earthquakes are shear dislocations on preexisting faults. To obtain successful results, it is necessary that the input dataset include at least four focal mechanisms of different orientations (Gephart and Forsyth, 1984).

The aim of the inversion is to determine the directions of the principal stress axes σ_1, σ_2, σ_3 ($\sigma_1 > \sigma_2 > \sigma_3$) and the shape factor $R = (\sigma_2 - \sigma_1)/(\sigma_3 - \sigma_1)$, which indicates the magnitude of σ_2 relative to σ_1 and σ_3. The best-fitting stress model is obtained when the angular difference (misfit) between the predicted and the observed fault plane and slip direction is minimum. The average misfit value of the best-fitting stress tensor indicates whether the assumption of stress uniformity in the investigated crustal volume is acceptable. According to Wyss *et al.* (1992), in homogeneous stress, errors in the data (focal mechanisms) on the order of 5°, 10°, and 15° were associated with misfit values not larger than 3°, 6°, and 8°, respectively. In our study the processing was carried out using the ZMAP software (Wiemer and Zuniga, 1994) and the weight given to each focal mechanism was based on its quality, which was derived during the focal-mechanism determination.

Applying the method to the whole dataset produced misfit errors that can only be explained by heterogeneity in the stress field. Thus we did not apply the technique to the whole area; instead, we divided our dataset into smaller parts, first according to the depth of the earthquakes and later based on the spatial distribution of the events and previous results on stress regime in the area (Kiratzi *et al.*, 1986). Figure 5 shows the three areas that were finally chosen and the corresponding lower-hemisphere plots of the *P* and *T* axes. Their distribution for the WMD and EMT areas shows
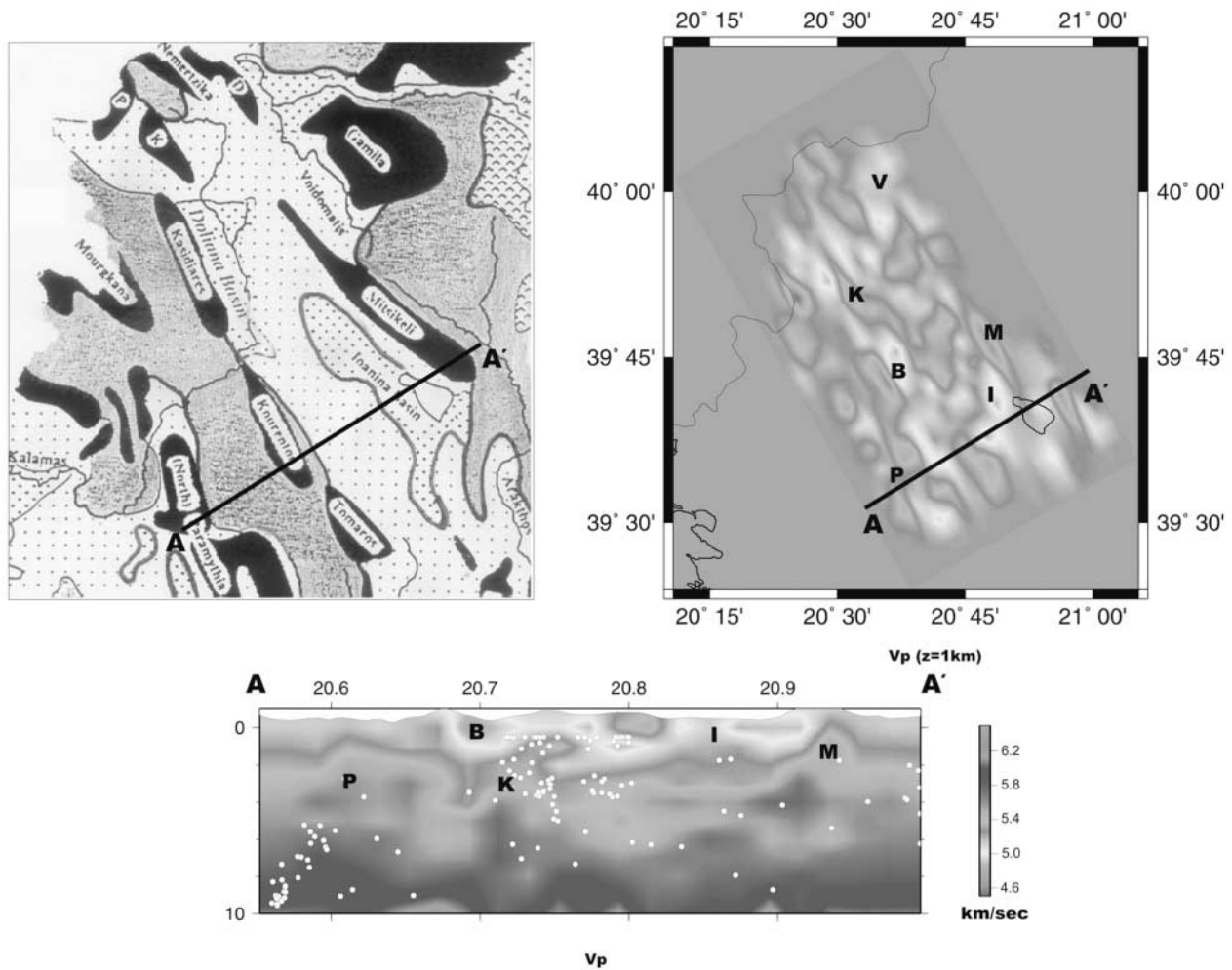
Figure 9. Comparison of main geological structures with results of passive tomography. P, Paramithia; B, Botsaras; K, Kourenton Kasidiaris; I, Ioanina plane; M, Mitsikeli; V, Voidomatis.

some clustering, but this is not so clear for the WMS area (Fig. 5). This is an indication that for the WMS area the stress field remains heterogeneous.

Stress Variations with Depth

The stress tensor was computed for two datasets (0–15 km and 15–30 km depth). The results of the analysis are presented in Table 2. For depths greater than 15 km (WMD) the σ_3 axis is almost vertical (dip of 60), whereas σ_1 is horizontal and has an azimuth of 203°. This stress-axis orientation supports compression in a northeast–southwest direction and corresponds well with the type of stress during the thrust movements and the present-day stress regime a few kilometers to the west along the coast, where collision is taking place. It seems that for these depths the stress field that produces the collision in the northwest coast of Greece affects the geodynamics further east. Other authors have proposed similar stress orientation for this area (Hatzfeld *et al.*, 1995; Papazachos and Kiratzi, 1996).

The derived stress field for the upper 15 km is far more complicated, with all the axes being subvertical. This supports the nonhomogeneous stress field for the whole Epirus. We could attribute the preceding stress orientation to a transpressional regime, which means that the type of faulting is reverse, oblique reverse, and strike slip.

Spatial Distribution of Stress

The stress-tensor results for the upper 15 km along with the spatial focal-mechanism distribution suggest that a further division of the shallow earthquakes dataset is necessary to obtain a well-constrained stress tensor. Thus, we divided our dataset using as a horizontal boundary the location of the internal Ionian thrust (Fig. 1), based on the clear change of faulting type east of this thrust where, almost pure normal fault-plane solutions were computed. The results for the two datasets (EMT, WMS) are presented in Table 1. The best stress model obtained for the EMT area has maximum compression σ_1 trending 182° and almost vertical (dip 67°),
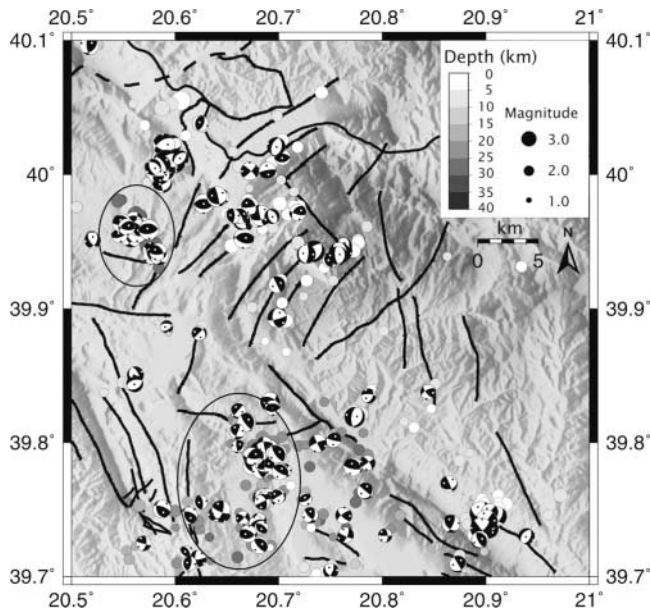
Figure 10.   Seismicity and focal mechanisms in the Ioannina basin and the Timfi area.

whereas minimum compression σ_3 trends 294° and is almost horizontal (dip 9°).

For the WMS area a different stress model was computed, with σ_1 almost horizontal and σ_3 close to vertical. Nevertheless, there is no clear compression in this area because the axis orientations are subvertical, so that this stress tensor could be attributed to a transpressional regime where both reverse and strike-slip faulting are taking place. This is clear in the field and has been noticed by other authors (Kiratzi *et al.*, 1986).

Discussion and Conclusions

During previous studies in the area of Epirus (IGSR and IFP, 1966; King *et al.*, 1983; Kiratzi *et al.*, 1987; IGMR, 1988; King *et al.*, 1993; Hatzfeld *et al.*, 1995, Waters, 1994) a few active structures were observed and the general characteristics of the seismicity distribution were pointed out.

Hatzfeld *et al.* (1995), based on microseismicity survey data from the broader area of northwestern Greece, proposed that seismicity is shallower than 40 km and is dipping toward the east. The authors described the seismicity pattern as of listric fault type and suggested that this pattern could be attributed to the reactivation of a former normal listric fault that now acts as a reverse fault. In our study, we have a different interpretation for this observation and attribute the change of focal depth to the combined effect of evaporite intrusion and deep seismic activity of the internal Ionian thrust. Thus, we interpret the absence of seismicity in the shallow part of the crust as due to the presence of an evaporite body with an inferred maximum thickness of 10 km. The seismicity-constrained evaporite thickness is in good agreement with analogous observations in Albania, a region

with geological history similar to Epirus. The evaporite crops out a few kilometers west of the internal Ionian thrust, where two small clusters of microseismicity north of Ioannina mark its presence in the subsurface (Figs. 3 and 4). As a result, the pattern of observed seismicity can be attributed to thrusts at a depth of 20 km that gradually reach the surface and to smaller structures of normal to oblique character close to the surface (Fig. 3b).

The stress regime in Epirus changes toward the east from compressional to extensional as suggested by King *et al.*, 1983; Kiratzi *et al.*, 1987; Papazachos and Kiratzi, 1996.

Our results show a stress change both in the horizontal and vertical directions. An extensional stress field was computed for the area east of the internal Ionian thrust (Fig. 11). Extension is taking place in a northeast–southwest direction perpendicular to the trend of the thrust belts. The computed stress distribution in the area is in very good agreement with that proposed by Kiratzi *et al.* (1987). They identified almost the same stress-axis orientations and attributed the observed stress pattern to collision and back-arc extension (Fig. 11). Regarding the area west of the internal Ionian thrust for shallow depths, the computed stress pattern is very complicated.

Table 2
Results of Stress-Tensor Inversion

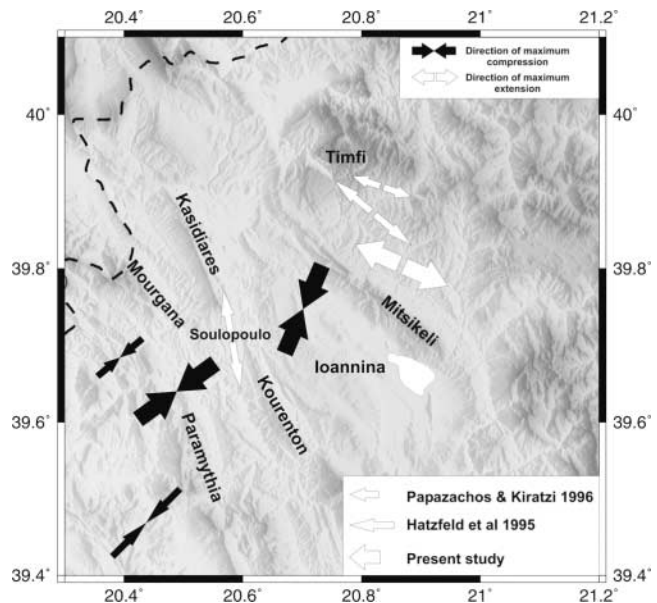| Area	σ_1 (dip/azimuth)	σ_2 (dip/azimuth)	σ_3 (dip/azimuth)	R	Misfit
EMT	67/182	21/27	9/294	0.5	10
WMS	25/54	26/157	53/287	0.8	12
WMD	10/203	28/299	60/95	0.5	9

Figure 11.   Comparison of stress axis orientations derived during this study with the results of Papazachos and Kiratzi (1996) and Hatzfeld *et al.* (1995).

Based on the relative orientations of the three major stress axes and the ratio *R*-value. we could propose a transpressional stress regime for this area. Finally, for the deeper part of the area west of the internal Ionian thrust the computed stress-axis orientations suggest a pure compressional regime in a northeast–southwest direction.

Based on the seismicity distribution and the stress-inversion results, we conclude that there is a clear change of the stress regime, just at the internal Ionian thrust, which seems to be the boundary between the transtensional regime in the east to transpressional at the west. We believe that evaporites have played an important role in this change through their intrusion under this thrust by providing the detachment surface that allows the change of tectonic deformation with increasing depth.

Acknowledgments

References

Amelung, F., and G. C. P. King (1997). Large scale tectonic deformations inferred from small earthquakes, *Nature* **386,** 702–705.

Aubouin, J. (1959). Contribution a l'etude geologique de la Gréce, septentrionale, les confins de l'Epire et de la Thessalie, *Ann. Géol. Pays. Hellen* **10,** 1–483.

Avramidis, P., A. Zelilidis, and N. Kontopoulos (2000). Thrust dissection control of deep-water clastic dispersal patterns in the Klematia—Paramythia foreland basin, western Greece, *Geol. Mag.* **137,** no. 6, 667–685.

Boccaletti, M., R. Caputo, D. Mountrakis, S. Pavlides, and N. Zouros (1997). Paleoseismicity of the Souli fault, Epirus, western Greece, *J. Geodyn.* **24,** 117–127.

Bott, M. H. P. (1959). The mechanics of oblique slip faulting, *Geol. Mag.* **96,** 109–117.

Deschamps, A., and G. C. P. King (1984). Aftershocks of the Campania-Lucania (Italy) earthquake of 23 November 1980, *Bull. Seism. Soc. Am.* **74,** no. 6, 2483–2517.

Doutsos, T., and I. Koukouvelas (1998). Fractal analysis of normal faults in northwestern Aegean area. *J. Geodyn.* **26,** 197–216.

Doutsos, T., N. Kontopoulos, and D. Fridas (1987). Neotectonic evolution of northwestern continental Greece, *Basin Res.* **1,** 177–190.

Gephart, J. (1990). Stress and the direction of slip on fault planes, *Tectonics* **9,** 845–858.

Gephart, J. W., and D. W. Forsyth (1984). An improved method for determining the regional stress tensor using earthquake focal mechanism: application to the San Fernando earthquake sequence, *J. Geophys. Res.* **89,** 9305–9320.

Hatzfeld, D., L. Kassaras, D. Panagiotopoulos, D. Amorese, K. Makropoulos, G. Karakaisis, and O. Coutand (1995). Microseismicity and strain pattern in northwestern Greece, *Tectonics* **14,** 773–785.

Institute for Geology Subsurface Research of Greece and Institute Francais de Petrole (IGSR and IFP) (1966). *Etude geologique de l'Epire*, Paris, Technip, 306 pp.

Institute of Geology and Mineral Resources (IGMR) (1967a). Geological map of Greece, Ioannina and Klematia sheet (1:50,000), Athens, Greece.

Institute of Geology and Mineral Resources (IGMR) (1967b). Geological map of Greece, "Filiates-Tsamadas" sheets (1:50,000), Athens.

Institute of Geology and Mineral Resources (IGMR) (1967c). Geological map of Greece, "Tsamadas" sheet (1:50,000), Athens.

Institute of Geology and Mineral Resources (IGMR) (1988). Seismotectonic map of Greece, Athens, Greece.

Jacobshagen, V. (1986). Geologie von Griechenland. Beiträse Zur Regionalen Geologie der Erde, **19,** Berlin.

King, G., D. Sturdy, and J. Whitney (1993). The landscape geometry and active tectonics of the northwest Greece, *Geol. Soc. Am. Bull.* **105,** 137–161.

King, G., A. Tselentis, J. Gomberg, P. Molnar, S. Roecker, H. Sinvhal, C. Soufleris, and J. Stock (1983). Microearthquake seismicity and active tectonics of northwestern Greece, *Earth Planet Sci. Lett.* **66,** 279–288.

Kiratzi, A., E. Papadimitriou, and B. C. Papazachos (1987). A microearthquake survey in the Steno dam site in northwestern Greece, *Ann. Geophys.* **592,** 161–166.

Kissling, E., W. L. Elsworth, D. Eberhart-Phillips, and U. Kradofler (1994). Initial reference models in seismic tomography, *J. Geophys. Res.* **99,** 19,635–19,646.

Lee, W. H. K., and J. C. Lahr (1975). HYPO71 (Revised): A computer program for determining hypocenter, magnitude, and first motion pattern of local earthquakes, *U.S. Geol. Surv. Open-File Rept. OF 85-749.*

Lee, W. H. K., and C. M. Valdes (1985). HYPO71PC A personal computer version of the HYPO71 earthquake location program, *U.S. Geol. Surv. Open-File Rept. OF 85-749.*

Lee, W. H. K., R. E. Bennet, and K. L. Meagher (1972). A method of estimating magnitude of local earthquakes from signal duration, *U.S. Geol. Surv. Open-File Rept. OF 1-28.*

Mercier, J., B. Bousquet, N. Delibasis, I. Drakopoulos, B. Keraurden, F. Lemell, and D. Sorel (1972). Deformations en compression dans le quartinaire des ravages Ioniens. Donnes neotectoniques et seismiques. *C. R. Acad. Sci. Paris* **275,** 2307–2310.

Papazachos, C., and A. Kiratzi (1996). A detailed study of the active crustal deformation in the Aegean and surrounding area, *Tectonophysics* **253,** 129–153.

Reasenberg, P., and D. Oppenheimer (1985). FPFIT, FPPLOT and FPPAGE: Fortran computer programs for calculating and displaying earthquake fault plane solutions, *U.S. Geol. Surv. Open-File Rept. OF 95-515*, 24 pp.

Taymaz, T., J. A. Jackson, and D. McKenzie (1991). Active tectonics of the north and central Aegean Sea, *Geophys. J. Int.* **106,** 433–490.

Thurber, C. H. (1986) Analysis methods for kinematic data from local earthquakes, *Rev. Geophys.* **24,** 793–805.

Tselentis, G.-A., N. Melis, E. Sokos, and K. Papatsimpa (1996). The Egion June 15, 1995 (6.2 ML) Earthquake, Western Greece, *Pure Appl. Geophys.* **147,** 83–98.

Underhill, J. R. (1989). Late Cenozoic deformation of the Hellenide foreland, western Greece, *Geol. Soc. Am. Bull.* **101,** 613–634.

Velaj, T., I. Davison, A. Serjani, and I. Alsop (1999). Thrust tectonics and the role of evaporites in the Ionian Zone of the Albanides, *AAPG Bull.* **83,** 1408–1425.

Waters, D. (1994). The tectonic evolution of Epirus, Northwest Greece, *Ph.D. thesis*, University of Cambridge, Cambridge, p. 248.

Wessel, P., and W. H. F Smith (1991). Free software helps map and display data, *EOS Trans. AGU* **72,** 441, 445–446.

Wiemer, S., and R. F. Zuniga (1994). ZMAP—a software package to analyze seismicity, *EOS Trans. AGU* **75,** Fall Meeting, 456.

Wyss, M., B. Liang, W. Taginawa, and W. Xiaopin (1992). Comparison of orientations of stress and strain tensor based on fault plain solutions in Kaoiki, Hawai, *J. Geophys. Res.* **97,** 4769–4790.

Laboratory of Seismology
University of Patras
Rio 26500, Patras
Greece
tselenti@upatras.gr
thimios@geology.upatras.gr
annaserp@geology.upatras.gr
  (G.-A.T., E.S., A.S.)

LandTech Enterprises
Ocean House Hunter Street
Cardiff Bay
CFIO SFR United Kingdom
nmartakis@landtechsa.com
  (N.M.)